

Scaling and glassy behavior in lamellar ordering

Aiguo Xu^(*) and G. Gonnella

Dipartimento di Fisica, Università di Bari

and Center of Innovative Technologies for Signal Detection and Processing (TIRES)

*and Istituto Nazionale per la Fisica della Materia and Istituto Nazionale di Fisica Nucleare, Sez. di Bari,
via Amendola 173, 70126 Bari, Italy*

A. Lamura

Istituto Applicazioni Calcolo, CNR, Sezione di Bari, via Amendola 122/D - 70126 Bari - Italy

(Dated: December 2, 2024)

We study the kinetics of domain growth of fluid mixtures quenched from a disordered to a lamellar phase. At low viscosities, when hydrodynamic modes become important, dynamical scaling is verified in the form $C(\vec{k}, t) \sim L^\alpha f[(k - k_M)L]$ where C is the structure factor with maximum at k_M and L is a typical length changing from power law to logarithmic growth at later times. The formation of grain boundary defects can explain this behavior of L . Applied shear flow alleviates frustration and gives power-law growth at all times.

PACS numbers: 64.75.+g; 05.70.Ln; 47.20.Hw; 82.35.Jk.

The kinetics of the growth of ordered phases after a quench from a disordered state continues to provide interesting physical questions. While the process is reasonably well understood for the case of binary mixtures, where dynamical scaling occurs and domains grow with power-law behavior [1], problems at fundamental level remain to be solved for more complex systems [2]. In this Letter we consider the case of fluid mixtures where, due to competing interactions, the system would arrange itself in stripes. Examples are di-block copolymer melts, where chains of type A and B, covalently bonded end-to-end in pairs, segregate at low temperatures in regions separated by a stack of lamellae [3], or ternary mixtures where surfactant form interfaces between oil and water [4]. Other systems with lamellar order are smectic liquid crystals [5], dipolar [6] and supercooled liquids [7], chemically reactive binary mixtures [8], doped Mott insulators [9], magnetic films [10]. Lamellar patterns are also observed in Raleigh-Bénard cells above the convective threshold [11].

The ordering of lamellar systems is characterized by the presence of frustration on large scales. This affects the late time evolution which, as discussed below, can be very slow or also frozen. Relations with the dynamics of structural glasses have been considered in recent literature [12, 13]. Our purpose here is to evaluate the role of hydrodynamics in this process. We consider a model, particularly appropriate for describing di-block copolymers, based on Ginzburg-Landau convection-diffusion and Navier-Stokes equations. Our results show that, when hydrodynamical modes are effective (at sufficiently low viscosities), dynamical scaling holds with a complex dependence of characteristic lengths on time, as in systems with quenched disorder [14]. Preasymptotic power-law behavior is followed by slower logarithmic growth or glassy behavior at later times. The ordering process is dominated by the dynamics of grain boundary defects be-

tween domains of differently oriented lamellae. The late time logarithmic behavior is interpreted as an activated growth induced by hydrodynamics. Applied shear flow alleviates frustration giving power-law behavior also at late times. We expect our findings to be relevant for a broad class of systems with lamellar order.

The model is based on the equilibrium free energy [15, 16]

$$\mathcal{F}\{\varphi\} = \int d^d x \left\{ \frac{a}{2} \varphi^2 + \frac{b}{4} \varphi^4 + \frac{\kappa}{2} |\nabla \varphi|^2 + \frac{c}{2} (\nabla^2 \varphi)^2 \right\} \quad (1)$$

where φ is the order parameter field representing the local concentration difference between the two components of the mixture. The parameters b and c have to be positive in order to ensure stability. For $a < 0$ and $\kappa > 0$ the two homogeneous phases with $\varphi = \pm \sqrt{-a/b}$ coexist. A negative κ favors the presence of interfaces and a transition into a lamellar phase can occur. In single mode approximation, assuming a profile like $A \sin k_0 x$ for the direction transversal to the lamellae, one finds ($|a| = b$) the transition at $a \approx -1.11\kappa^2/c$ where $k_0 = \sqrt{-\kappa/2c}$, $A^2 = 4(1 + \kappa^2/4cb)/3$. The expression (1) can be also written for negative κ as $\mathcal{F}\{\varphi\} = \int d^d x \left\{ \frac{\tau}{2} \varphi^2 + \frac{b}{4} \varphi^4 + \frac{c}{2} [(\nabla^2 + k_0^2) \varphi]^2 \right\}$, $\tau = a - ck_0^4$, and in this form is generally used to describe di-block copolymers in the weak segregation limit [16].

The dynamical equations are [2]

$$\frac{\partial v_\alpha}{\partial t} + \vec{v} \cdot \vec{\nabla} v_\alpha = -\frac{1}{\varrho} \frac{\partial P_{\alpha\beta}}{\partial x_\beta} + \nu \nabla^2 v_\alpha \quad , \quad (2)$$

$$\frac{\partial \varphi}{\partial t} + \vec{\nabla} \cdot (\varphi \vec{v}) = \Gamma \nabla^2 \frac{\delta \mathcal{F}}{\delta \varphi} \quad , \quad (3)$$

where v_α are the components of the velocity field, ϱ is the total density of the mixture and the incompressibility condition $\vec{\nabla} \cdot \vec{v} = 0$ is considered. ν is the kinematic

FIG. 1: Configurations at different times of a portion 256×256 of the lattice.

viscosity and Γ is a mobility coefficient. The pressure tensor is the sum of the usual hydrodynamical part and of a tensor $P_{\alpha\beta}^{chem}$ depending on φ , obtainable from the free energy and containing off-diagonal terms, whose expression can be found in [17]. The laplacian in the r.h.s. of Eq. (3) ensures the conservation of the order parameter. We will simulate these equations using a finite difference scheme for the convection-diffusion equation and a Lattice Boltzmann Method (LBM) for the Navier-Stokes equation. Advantages of this method [18] with respect to other LBM schemes for fluid mixtures are that spurious terms appearing in Eq.(3) [19] are avoided and the numerical efficiency is increased. We will restrict to the two-dimensional case.

We can summarize now what is known on the ordering properties of lamellar fluids. Previous studies of the full model (1-3) [17], without quantitative analysis due to the small size of the lattice considered, showed that the effects of hydrodynamical modes are crucial for obtaining well ordered domains on large scales. More results exist for variants of the model (1) with long-range interactions, without hydrodynamics [20, 21, 22] or neglecting the inertial terms of the l.h.s. of Eq.(2) [23]. Eq.(3) without advection and with non-conserved order parameter, corresponding to the Swift-Hohenberg model for Raleigh-Bénard convection [24, 25, 26, 27, 28], has been also largely studied. Regimes with dynamical scaling have been found with the order parameter structure factor behaving as $C(\vec{k}, t) \equiv \langle |\varphi_{\vec{k}}(t)|^2 \rangle \sim t^z f[(k - k_0)t^z]$, $\varphi_{\vec{k}}(t)$ being the Fourier transform of $\varphi(\vec{x}, t)$. However,

also in the above cases, mostly related to Eq.(3) only, the situation is not completely clear. Different values of the growth exponent z ranging from $1/5$ to $1/4$ [21, 23, 25, 26, 27, 29, 30, 31] and $1/3$ [28] were found depending on the steepness of the potential in (1). Slower evolution with frozen states and grain boundary pinning has been also observed [12, 27] for deeper quenches.

We run our simulations on a 1024^2 square lattice starting from disordered configurations. We fixed $|a| = b$ so that the minimum of the potential part of the free-energy is at $\varphi = \pm 1$. We checked on small systems (128^2) for different κ in the lamellar phase that the expected equilibrium state was reached. No significant differences with respect to the single-mode approximation were found. The value of c was fixed in such a way that the period is about 10 times the lattice spacing and $|a| = 2 \times 10^{-4}$, $\kappa = -3 \times |a|$, $c = 3.8 \times |a|$, $\Gamma = 25$ for all cases presented. Details on the LBM part of the code can be found in [32]. Different time steps were used for the discretization of Eq.(3) and for the lattice Boltzmann equation [18].

After the quench, lamellae start to form evolving until the equilibrium wavelength is locally reached. This part of the ordering process does not depend on the value of viscosity. Later, however, the system continues to order only at sufficiently low viscosities ($\nu \lesssim 0.1$). Otherwise, local defects dominate [17] and, at times of order $t \sim 3000$, the system results frozen in tangled configurations. An example of evolution at low viscosity ($\nu = 8.33 \times 10^{-3}$) is shown in Fig.1. Different kinds of defects can be observed. The annihilation of a couple of dislocations, approaching each other with constant velocity, is put in evidence. Order on larger scales can be observed at the last time of the figure.

A quantitative description of the ordering process comes from the analysis of the structure factor $C(\vec{k}, t)$. After spherical average we plotted $C(k, t)$ at different times. In the early regime, with $t \lesssim 3000$, $C(k, t)$ develops a maximum at a momentum k_M which decreases with time until the equilibrium value k_0 is reached. Then the peak of $C(k, t)$, remaining at k_0 , continues to grow while the width decreases indicating an increase of order in the system. A characteristic length L for this process can be extracted from the structure factor in the usual way [23] by measuring the full width δk of C at half maximum and defining $L(t) = 2\pi/\delta k$. In the inset of Fig.2 we plotted on log-log scale $L(t)$, calculated by averaging over 5 different runs. For about one decade a power-law behavior $L \sim t^z$ can be observed with $z = 0.30 \pm 0.02$. The growth becomes slower at later times and, indeed, we find $L \sim \ln t$ as the straight line in the main frame of Fig.2 suggests. We checked that the slowing down cannot be attributed to finite size effects; indeed, at the latest times considered, $L(t)$ is less than 1/10 of the size of the system.

In order to verify dynamical scaling the behavior of

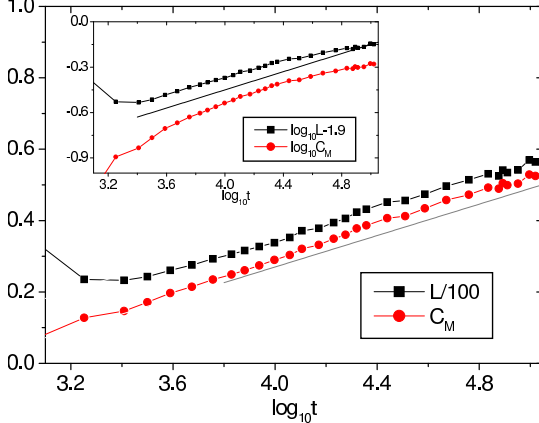


FIG. 2: Time behavior of characteristic size L and $C_M \equiv C(k_M, t)$ on log-log (inset) and log-linear scales. The straight line in the inset has slope 0.3.

the peak $C_M \equiv C(k_M, t)$ of the structure factor was also analyzed. From Fig.2 one sees that C_M grows similarly to $L(t)$ but with a different rate. This suggests to consider scaling behavior in the general form $C(k, t) \sim L^\alpha f[(k - k_M)L]$ [33]. This differs from the usual expression considered in lamellar ordering ($C \sim t^z f[(k - k_M)t^z]$) due to the introduction of α and the use of L even if not given by a power law. As illustrated in the inset of Fig.3, we evaluated $\alpha = 1.25$. Then, by using this value, we found, as shown in Fig.3, that rescaled structure factors overlap at all times, after $t \sim 3000$, on a single curve confirming our scaling assumption and suggesting an analogy with kinetic behavior in systems with quenched disorder. In Random Field Ising Models (RFIM), for example, diffusive growth changes over to logarithmic behavior but dynamical scaling holds at all times with the same scaling function as in standard Ising model [14].

The growth behavior of L can be explained as following from the motion of extended defects (grain boundaries) through a background of curved stripes. These defects separate domains of different oriented lamellae and can be recognized in Fig.1. Boyer and Viñals [12], in the context of the Swift-Hohenberg model, were able to obtain an equation for the motion of a grain boundary at position x_{gb} . They found $\dot{x}_{gb} = AC^2(t) - B \cos(2k_0 x_{gb} + \phi)$ where C is the curvature of lamellae parallel to the boundary and A, B, ϕ are model-dependent parameters. Assumption of dynamical scaling gives a growth like $t^{1/3}$ until a critical curvature is reached. At this point, in absence of other processes, defects would be pinned and the system frozen. We expect that the arguments of [12] also hold in our case with the velocity field acting as a perturbation in the grain boundary equation. The power-law behavior of Fig.2 is compatible with this argument and the later logarithmic growth can be interpreted as an activated growth induced by the velocity field.

To our knowledge this is the first time that dynamical scaling with power-law behavior followed by logarithmic growth is found in systems without quenched disorder. This is interesting also in relation with the existence of

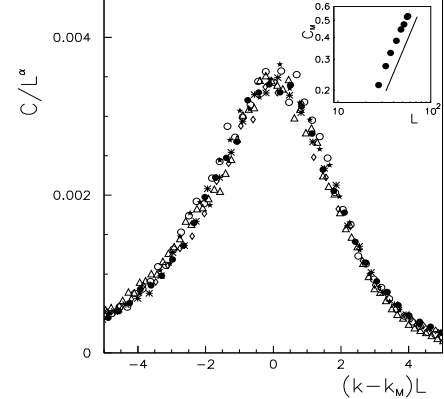


FIG. 3: Rescaled structure factors at different times. Symbols $\triangle, \circ, \star, *, \diamond$ refer to times 4600, 14100, 40800, 61100, 78100, 123100, respectively. In the inset C_M is plotted on log-log scale as a function of L ; the slope of the line is 1.25.

an equilibrium glass transition in systems with lamellar order [13]. Concerning the exponent α , its value is related to the compactness of domains and is $\alpha = D$ in asymptotic growth of binary mixtures, $\alpha = 0$ in early time regime when interfaces are forming [33]. Our results with $\alpha > 1$ show that the argument for $\alpha = 1$ based on the existence of only 1 scaling dimension for $D = 2$ lamellar systems [25] does not hold in presence of hydrodynamics. A renormalization group analysis, to be reported elsewhere, can relate α to a not trivial value of the scaling dimension of the fixed point hamiltonian.

We also studied lamellar ordering in presence of shear flow. Shear was applied with bounce-back conditions on rigid walls moving with velocity $\pm v_{wall}$ at the top and bottom of the simulation volume [32]. Ordering is favored since interfaces want to orientate with the flow [34]. Breaking and recombination of domains, induced by shear, makes the elimination of topological defects faster too [35]. As a result, logarithmic growth disappears and ordering occurs also asymptotically with power-law behavior even in cases, at high viscosity, where without shear freezing would have been observed.

In Fig.4 an example of evolution at low viscosity ($\nu = 0.03$, others parameter as before) is shown. This case is peculiar since characterized by the formation of long grain boundaries in the direction of the flow. The band with vertical lamellae disappears at late times when the system becomes completely horizontally oriented. This effect can be related to the particular patterns of the velocity field at this viscosity. Indeed, the time required for developing a linear velocity profile, roughly proportional to ν^{-1} [32], can be very large at low viscosities so that the imposed flow, for a large part of the simulation, is effective only close to the walls determining the anisotropy observed. At higher viscosities ($\nu \gtrsim 1$), the ordering of the system proceeds more obviously with lamellae following everywhere the direction of the flow. Growth was measured by the quantities $L_\alpha = \int d\vec{k} C(\vec{k}, t) / \int d\vec{k} |k_\alpha| C(\vec{k}, t)$ ($\alpha = x, y$). In Fig.5 a typical case ($\nu = 7.5$) is shown. As announced, a power law behavior for L_x is found with

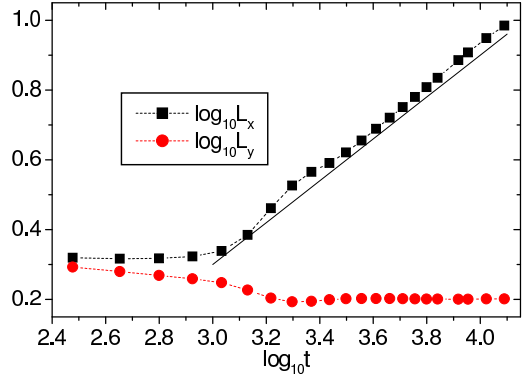


FIG. 4: Configurations at different times of the central part (684^2) of a 1024^2 lattice at $\nu = 0.03$. Shear rate is $\dot{\gamma} = 10^{-3}$.

exponent $z_x = 0.6$ while L_y relaxes to the equilibrium value. Similar results were found for other values of ν ; a detailed exposition of our results with shear will appear elsewhere.

To conclude, we have studied lamellar ordering in fluid mixtures with competitive interactions. At low viscosities, when hydrodynamic modes are effective, dynamical scaling holds in the form $C(\vec{k}, t) \sim L^\alpha f[(k - k_M)L]$ where L is a characteristic length changing from power law to logarithmic growth at later times. This scaling, also found in systems with quenched disorder, is a new result for systems where frustration is dynamically generated. Shear flow removes grain boundary defects giving power-law behavior also at late times.

We warmly thank G. Amati, F. Corberi, F. Massaioli, E. Orlandini, M. Zannetti and J. Yeomans for helpful discussions. We acknowledge support by MIUR (PRIN-2002).

(*) Present address: Dept. of Physics, Yoshida-south Campus, Kyoto University, Sakyo-ku, Kyoto, 606-8501 Japan.

- [1] See, e.g., A. J. Bray, *Adv. Phys.* **43**, 357 (1994).
- [2] See, e.g., J.M. Yeomans, *Ann. Rev. Comput. Phys.* VII, 61 (2000).
- [3] F.S. Bates and G. Fredrickson, *Ann. Rev. Phys. Chem.* **41**, 525 (1990).
- [4] G. Gompper and M. Schick, *Phase transitions and critical phenomena* vol. **16** (Academic, New York, 1994).
- [5] See, for example, P. de Gennes, *The Physics of Liquid Crystals* (Clarendon, Oxford, 1974).
- [6] C. Roland and R. C. Desai, *Phys. Rev. B* **42**, 6658 (1990).
- [7] D. Kivelson, S. A. Kivelson, X. Zhao, Z. Nussinov, and G. Tarjus, *Physica A* **219**, 27 (1995); M. Grousson, V. Krakoviack, G. Tarjus, and P. Viot, *Phys. Rev. E* **66**, 026126 (2002)
- [8] S. C. Glotzer, E. A. Di Marzio, and M. Muthukumar, *Phys. Rev. Lett.* **74**, 2034 (1995).

FIG. 5: Evolution of L_x and L_y for $\dot{\gamma} = 10^{-4}$. The straight line has slope 0.6. At the latest times of the figure the system is almost completely ordered.

- [9] J.H Cho, F.C. Chou, and D.C. Johnston, *Phys. Rev. Lett.* **70**, 222 (1993).
- [10] K. De'Bell, A.B. MacIsaac, J.P. Whitehead, *Rev. Mod. Phys.* **72** 225 (2000).
- [11] M. C. Cross and P. C. Hohenberg, *Rev. Mod. Phys.* **65**, 851 (1993).
- [12] D. Boyer and J. Viñals, *Phys. Rev. E* **65**, 046119 (2002).
- [13] J. Schmalian and P.G. Wolynes, *Phys. Rev. Lett.* **85**, 836 (2000); M. Grousson, G. Tarjus, and P. Viot, *ib.* **86**, 3455 (2001).
- [14] M. Rao and A. Chakrabarti, *Phys. Rev. Lett.* **71**, 3501 (1993).
- [15] S. A. Brazovskii, *Sov. Phys. JETP* **41**, 85 (1975).
- [16] L. Leibler, *Macromolecules* **13**, 1602 (1980); T. Ohta and K. Kawasaki, *ib.* **19**, 2621 (1986); G.H. Fredrickson and E. Helfand, *J. Chem. Phys.* **87**, 697 (1987).
- [17] G. Gonnella, E. Orlandini, and J. Yeomans, *Phys. Rev. Lett.* **78**, 1695 (1997); *Phys. Rev. E* **58**, 480 (1998).
- [18] Details about the method will appear elsewhere.
- [19] M.R. Swift, E. Orlandini, W.R. Osborn, and J.M. Yeomans, *Phys. Rev. E* **54**, 5041 (1996).
- [20] F. Liu and N. Goldenfeld, *Phys. Rev. A* **39**, 4805 (1989).
- [21] Y. Shiwa, T. Taneike, and Y. Yokojima, *Phys. Rev. Lett.* **77**, 4378, (1996).
- [22] N.M. Maurits, A.V. Zvelindovsky, G.J.A. Sevink, B.A.C. van Vlimmeren, and J.G.E.M. Fraaije, *J. Chem. Phys.* **108**, 9150 (1998).
- [23] Y. Yokojima and Y. Shiwa, *Phys. Rev. E* **65**, 056308 (2002).
- [24] J. Swift and P. C. Hohenberg, *Phys. Rev. A* **15**, 319 (1977).
- [25] K. R. Elder, J. Viñals, and M. Grant, *Phys. Rev. Lett.* **68**, 3024 (1992).
- [26] M.C. Cross and D.I. Meiron, *Phys. Rev. Lett.* **75**, 2152 (1995).
- [27] Q. Hou, S. Sasa, and N. Goldenfeld, *Physica A* **239** 219 (1997).
- [28] D. Boyer and J. Viñals, *Phys. Rev. E* **64**, 050101(R) (2001).
- [29] J.J. Christensen and A.J. Bray, *Phys. Rev. E* **58**, 5364 (1998).
- [30] H. Qian and G.F. Mazenko, *Phys. Rev. E* **67**, 036102 (2003).
- [31] C. Harrison *et al.*, *Science* **290**, 1558 (2000); *Phys. Rev. E* **66**, 011706 (2002).
- [32] Aiguo Xu, G. Gonnella, and A. Lamura, *Phys. Rev. E*

67, 056105 (2003).

[33] A. Coniglio, P. Ruggiero, and M. Zannetti, Phys. Rev. E **50**, 1046 (1994).

[34] See, e.g., A. Onuki, J. Phys.: Cond. Matt. **9**, 6119 (1997).

[35] F. Corberi, G. Gonnella, and A. Lamura, Phys. Rev. Lett. **83**, 4057 (1999); ib. **81**, 3852 (1998).

This figure "fig1.jpg" is available in "jpg" format from:

<http://arxiv.org/ps/cond-mat/0404205v1>

This figure "fig4.jpg" is available in "jpg" format from:

<http://arxiv.org/ps/cond-mat/0404205v1>